

X-ray ionization yields and energy spectra in liquid argon

A. Bondar,^{a,b} A. Buzulutskov,^{a,b,*} A. Dolgov,^b L. Shekhtman,^{a,b} A. Sokolov^{a,b}

^a*Budker Institute of Nuclear Physics SB RAS, Lavrentiev avenue 11, 630090 Novosibirsk, Russia*

^b*Novosibirsk State University, Pirogov street 2, 630090 Novosibirsk, Russia*

E-mail: A.F.Buzulutskov@inp.nsk.su

ABSTRACT: The main purpose of this work is to provide reference data on X-ray ionization yields and energy spectra in liquid Ar to the studies in the field of Cryogenic Avalanche Detectors (CRADs) for rare-event experiments, based on noble-gas liquids. We present the results of two related researches. First, the X-ray recombination coefficients in the energy range of 10-1000 keV and ionization yields at different electric fields are determined in liquid Ar, based on the results of a dedicated experiment. Second, the energy spectra of pulsed X-rays in liquid Ar in the energy range of 15-40 keV, obtained in given experiments including that with the two-phase CRAD, are interpreted and compared to those calculated using a dedicated computer program, to correctly determine the incident X-ray energy. The X-ray recombination coefficients and ionization yields have for the first time been presented for liquid Ar in systematic way.

KEYWORDS: X-ray recombination coefficients and ionization yields in liquid argon; X-ray energy spectra in liquid argon.

*Corresponding author.

Contents

1. Introduction	1
2. Experimental procedures	2
3. Ionization yields	5
4. Energy spectra	9
5. Conclusions	11
6. Acknowledgements	11
References	11

1. Introduction

The main purpose of this work is to provide reference data on X-ray ionization yields and energy spectra in liquid Ar to the studies in the field of rare-event experiments based on noble-gas liquids. In particular, our group have a long-term activity in the field of two-phase Cryogenic Avalanche Detectors (CRADs) for dark matter search and coherent neutrino-nucleus scattering experiments [1] and their energy calibration [2],[3]. In the course of these developments [3],[4],[5],[6],[7],[8],[9],[10],[11],[12], two X-ray sources were constantly used to produce ionization in liquid Ar and Xe: a 59.5 keV X-ray line of the ^{241}Am radioactive source and the original pulsed X-ray tube with X-ray energies of 15-40 keV (0,11BSV7-Mo, [9],[13]). For many years these X-ray sources were successfully used to measure physical quantities characterizing CRAD performances in Ar and Xe: the charge gain [4],[5],[6],[7],[11], the spatial resolution [12], the scintillation light yield in the Near Infrared [6],[7],[9],[10] and the ionization yield of nuclear recoils [3].

On the other hand, the X-ray ionization yields and energy spectra in liquid Ar, often referred to in our previous and current works, have not been properly reflected in the literature. In this report we fill this gap, namely we present the results of two related researches in the field. First, the X-ray recombination coefficients in the energy range of 10-1000 keV and ionization yields at different electric fields are determined in liquid Ar, based on the results of a dedicated experiment. Second, the energy spectra of pulsed X-rays in liquid Ar measured in given experiments, in the energy range of 15-40 keV, are interpreted and compared to those calculated using a dedicated computer program, to correctly determine the incident X-ray energy.

It should be remarked that while the data on X-ray energy spectra are given here mostly for the reference purposes, the data on the recombination coefficients and ionization yields presented in the current work have a scientific novelty. Indeed, in contrast to Xe, little has been known so far about the X-ray ionization yield in liquid Ar at energies below 500 keV [2]. Accordingly, these data might be of particular interest for the energy calibration of dark matter and neutrino detectors using liquid Ar detection medium.

2. Experimental procedures

Fig. 1 shows schematic views of two experimental setups to perform the two studies discussed above. The left panel presents a dedicated liquid Ar ionization chamber, to measure the ionization yield at lower energies using a pulsed X-ray tube. The right panel presents a two-phase CRAD in Ar with THGEM/GAPD-matrix charge/optical readout, to measure its amplitude and coordinate characteristics, where either a pulsed X-ray tube or a 60 keV X-ray line from the ^{241}Am source was used to provide ionization in liquid Ar induced by X-rays of certain energies. The latter experimental setup was identical to that of ref. [12] where the first results on the performance of the combined multiplier composed of THGEMs [14] and a matrix of Geiger-mode APDs (GAPDs, [15]) in the two-phase CRAD were presented; the setup photograph is shown in Fig. 2. As concerns cryogenics and high and low voltage supply, the setups were similar to those described elsewhere [10],[11],[12]. Each experimental setup consisted of a 9 l vacuum-insulated cryogenic chamber filled with liquid Ar. The electron lifetime in the liquid was above 15 μs , which corresponds to the oxygen-equivalent impurity content below 30 ppb. The measurements were conducted at 87 K either in liquid Ar, in the first setup (Fig. 1, left), or two-phase Ar, in the second setup (Fig. 1, right).

In both experimental setups, the pulsed X-rays were produced by a pulsed X-ray tube with Mo anode (0,11BSV7-Mo, [13]). The tube was operated at a voltage of 40 kV and an anode current of 2.5 mA in a pulsed mode with a frequency of 240 Hz. The latter was provided by a gating grid, which was gated by a dedicated pulse generator. The pulse generator also provided a trigger for reading out the data. The cryogenic chamber was irradiated from outside practically uniformly across the active area, through a collimator and two aluminium windows at the chamber bottom, each 1 mm thick and of a diameter of 5 cm.

In the first experimental setup, the pulsed X-rays reached the liquid Ar ionization gap after

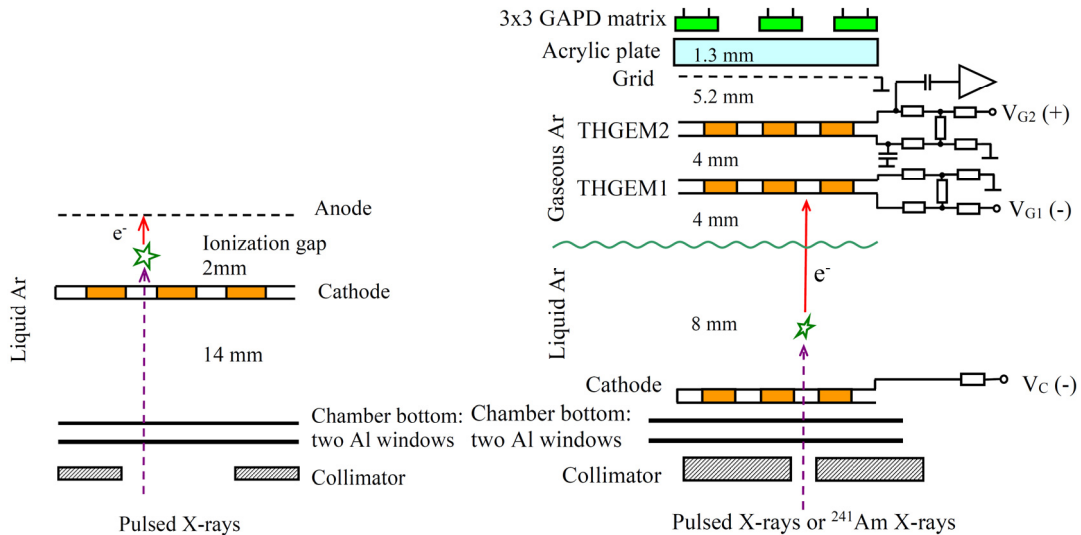


Fig. 1. Left: schematic view of a dedicated liquid Ar ionization chamber to measure the X-ray ionization yield. Right: schematic view of a two-phase CRAD in Ar with THGEM/GAPD-matrix charge/optical readout to study its amplitude and coordinate characteristics [12].

passing through a 14 mm thick liquid Ar layer, the latter acting as an additional X-ray filter to the two Al input windows: see Fig. 1 (left). In the second experimental setup, the pulsed X-rays reached the cathode gap after passing through a THGEM-plate electrode, 0.5 mm thick, laying on the chamber bottom and acting as a cathode. This electrode was equivalent to the additional X-ray filter consisted of 0.5 mm thick liquid Ar layer within the THGEM holes; the rest of the THGEM area worked as much harder X-ray filter due to copper cladding and thus might be ignored.

The appropriate spectra of X-rays reaching the sensitive volume, the ionization gap in the first setup and the cathode gap in the second setup, were calculated using a dedicated computer program [16]; they are shown in Fig. 3. For comparison, that of filtering with 2 mm thick liquid Ar in addition to the two Al windows, is also shown. One can see that the average energy of incident X-rays after filtering amounts to 35 keV in the first setup and 25 keV in the second setup. In section 4 the latter spectrum will be compared to that obtained in experiment.

In the first experiment setup (Fig. 1, left), the X-ray pulse had a sufficient power to provide measurable ionization charge, normally having values of tens of thousands electrons in liquid Ar. In addition, it was sufficiently fast, having a width of 0.5 μ s, to provide a reasonable time resolution. The ionization signal was recorded in the ionization chamber (parallel-plate gap) with an active area of 30 \times 30 mm² and thickness of 2 mm. The gap was formed by a THGEM-plate electrode and a wire grid as shown in Fig. 1 (left). The charge (ionization) signal was read out from the anode electrode using a charge-sensitive preamplifier followed by research amplifier with an overall shaping time of 10 μ s, with the electronic noise corresponding to the Equivalent Noise Charge of $\sigma=500$ e. The amplifiers were placed outside the cryogenic chamber. The signals were digitized and memorized for further off-line analysis with a TDS5032B digital oscilloscope, by the trigger provided by the X-ray tube pulse generator.

In the second experimental setup (Fig. 1, right and Fig. 2), the cryogenic chamber included a cathode electrode, immersed in a \sim 1 cm thick liquid Ar layer, and a double-THGEM multiplier with an active area of 10 \times 10 cm², placed in the gas phase above the liquid and optically read out by a 3 \times 3 matrix of GAPDs in the NIR. The cathode and THGEM electrodes were biased through a resistive high-voltage divider, placed outside the cryostat. In all the measurements, the electric field within liquid Ar was kept at 1.76 kV/cm. In case of the pulsed X-ray irradiation, a steel cylindrical collimator with a hole diameter of 2 mm and thickness of 10 mm was used. In addition to the pulsed X-rays, the detector could be irradiated from outside by X-rays from a ²⁴¹Am source providing a 60 keV line and lower energy lines, at a rate of a few Hz. The charge signal was recorded from the last electrode of the second THGEM using a charge-sensitive preamplifier followed by research amplifier with an overall shaping time of 10 μ s (similarly to the first setup). The DAQ system included an 8-channel Flash ADC CAEN V1720 (12 bits, 250 MHz): the optical signals from 7 GAPDs (after the fast amplifiers) and the charge signal from the double-THGEM multiplier were digitized and stored in a computer for further off-line analysis.

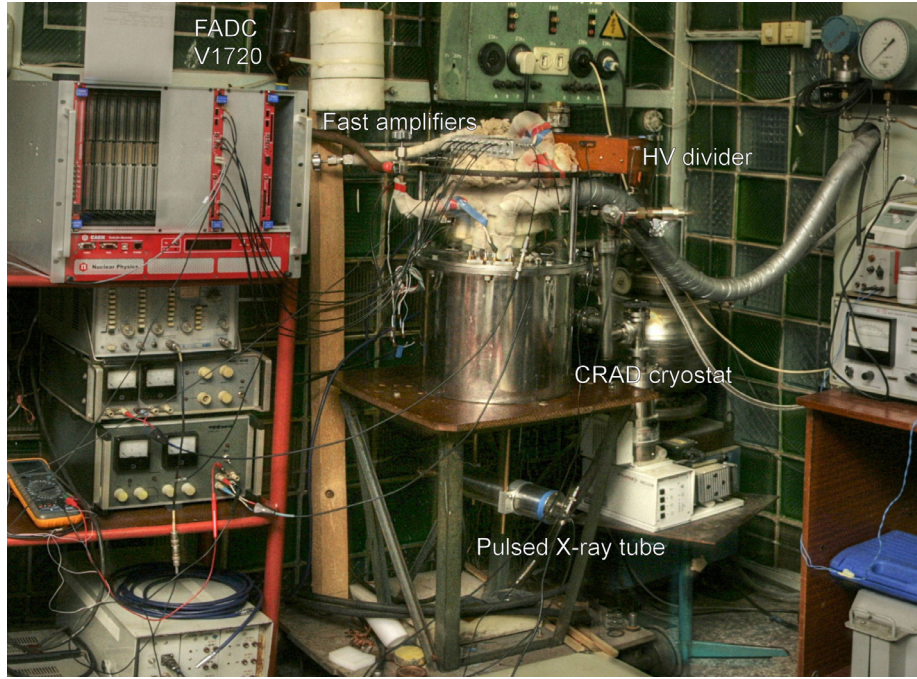


Fig. 2. Photograph of the two-phase CRAD in Ar with THGEM/GAPD-matrix charge/optical readout of Fig. 1 (right) [12]. The CRAD cryostat, pulsed X-ray tube, HV divider box, fast amplifiers box and flash ADC module V1720 in the VME crate of the DAQ system are indicated in the figure.

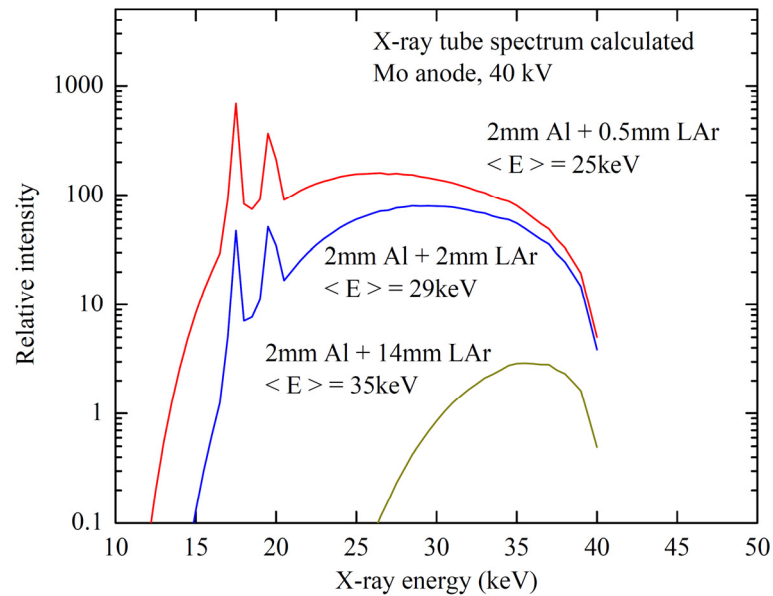


Fig. 3. Calculated spectra of pulsed X-rays reaching either the ionization gap of the liquid Ar ionization chamber or the cathode gap of the two-phase CRAD of Fig. 1 (left) and (right) respectively, i.e. after filtering with 2 mm thick Al windows and with either 14 or 0.5 mm thick liquid Ar layer. For comparison, that of filtering with 2 mm thick Al windows and 2 mm thick liquid Ar layer is shown.

3. Ionization yields

The ionization yield from a track of a particle absorbed in or passing through the noble-gas liquid (Q_y) is defined as follows:

$$Q_y = n_e / E_0 \quad . \quad (1)$$

Here n_e is the number of electrons escaping recombination with positive ions; it depends on the nature of the particle collision with atoms (electron or nuclear recoils), on the energy deposited by a particle in the liquid (E_0) and on the electric field in the liquid (\mathcal{E}). n_e is always smaller than the initial number of ion pairs produced in the liquid by a particle (N_i). In the absence of a complete recombination model, it is generally accepted that the following parametrization works well [2],[17],[18]:

$$n_e = N_i / (1 + k/\mathcal{E}) \quad , \quad (2)$$

where k is a fitting constant, often called recombination coefficient. These equations are valid for both electron recoils, induced by electron or gamma-ray irradiation, and nuclear recoils.

In this section, we determine the recombination coefficients and ionization yields induced by X-ray absorption in liquid Ar for the energies and electric fields relevant to our previous [3],[12] and future [19],[20] studies, in particular in the energy range of 10-1000 keV. The data on the X-ray ionization yields in liquid Ar at an electric field of 2.3 kV/cm have been already used in ref. [3], to calibrate the ionization charge scale when measuring the ionization yield of nuclear recoils in liquid Ar. In addition, the similar data will be used in our forthcoming publications on the performance of the two-phase CRAD with THGEM/GAPD-matrix multiplier [19] and that with electroluminescence gap [20], at a field of 1.76 kV/cm and 0.6 kV/cm respectively. Accordingly, in this section we determine the X-ray ionization yields in liquid Ar for the electric field values of 0.6, 1.75 and 2.3 kV/cm, using the energy dependence of the ionization yields in the energy range of 10-1000 keV.

To determine this energy dependence one should know in turn the recombination coefficients at several energy points. While for liquid Xe there are enough data on the recombination coefficients in the energy range of interest [2],[17],[21],[22],[23] and on those of ionization yield [24],[25], little was known about those in liquid Ar [22],[26],[27]. This is seen from Table 1 showing the recombination coefficients in liquid Ar and Xe for X-ray- or electron-induced ionization. This is also seen from Fig. 4 showing the relative ionization yields in liquid Ar and Xe, calculated from Eq. (2) using those recombination coefficients, as a function of the X-ray or electron energy, at an electric field of 1.75 kV/cm. Here all the Xe recombination coefficients and that of Ar at 976 keV are reproduced from Table 2.6 of ref. [17]. The recombination coefficient for Ar at 364 keV was obtained by ourselves from the data of ref. [26]. One can see that the ionization yield decreases monotonically with decreasing energy.

It should be remarked that we deliberately ignore here the low-energy region, below 10 keV, since the energy dependence of the ionization yield below this energy might change its character: in particular in liquid Xe, at further energy decrease a minimum is predicted first, and then the growth of the yield [24],[25].

Liquid	X-ray or electron energy E_0 (keV)	Recombination coefficient k (V/cm)	Reference
Ar	35	1820±110	This work
Ar	364	584±40	Deduced from [26]
Ar	976	560±10	[22]
Xe	15.3	2370±150	[21]
Xe	17.3	2100±300	[21]
Xe	21.4	1800±80	[21]
Xe	550	410±30	[22]
Xe	662	420±30	[23]

Table 1. Recombination coefficients in liquid Ar and Xe for X-ray- or electron-induced ionization in the energy range of 10-1000 keV. The Xe recombination coefficients and that of Ar at 976 keV are reproduced from Table 2.6 of ref. [17].

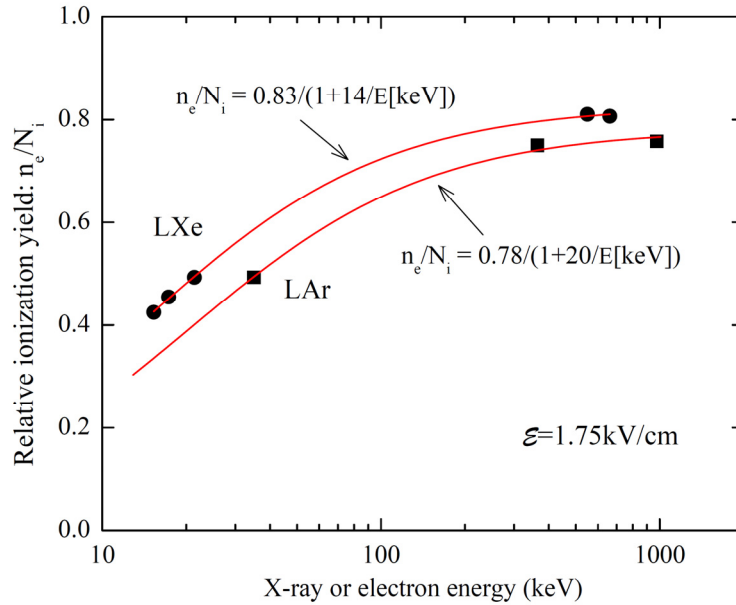


Fig. 4. Relative ionization yields in liquid Ar and Xe for electron recoils, due to X-ray or electron irradiation, as a function of the X-ray or electron energy, at an electric field of 1.75 kV/cm.

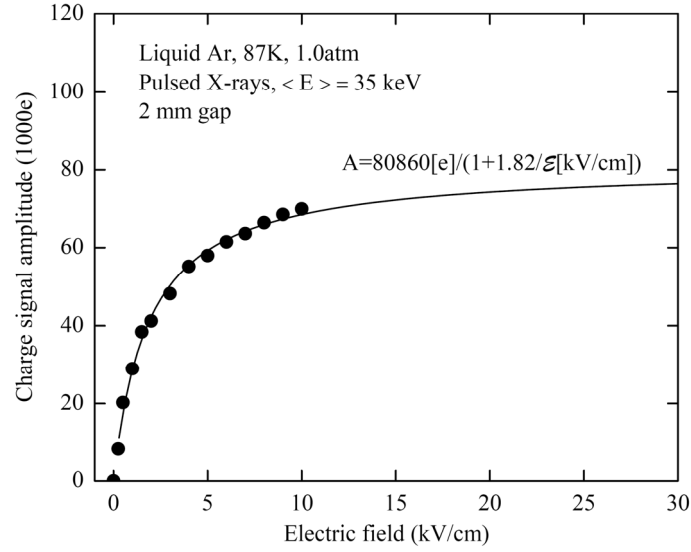


Fig. 5. Anode signal charge expressed in electrons, per X-ray pulse, as a function of the electric field in the liquid Ar ionization chamber of Fig. 1 (left), produced by pulsed X-rays with the average energy of 35 keV. The curve is the recombination model fit to the data points.

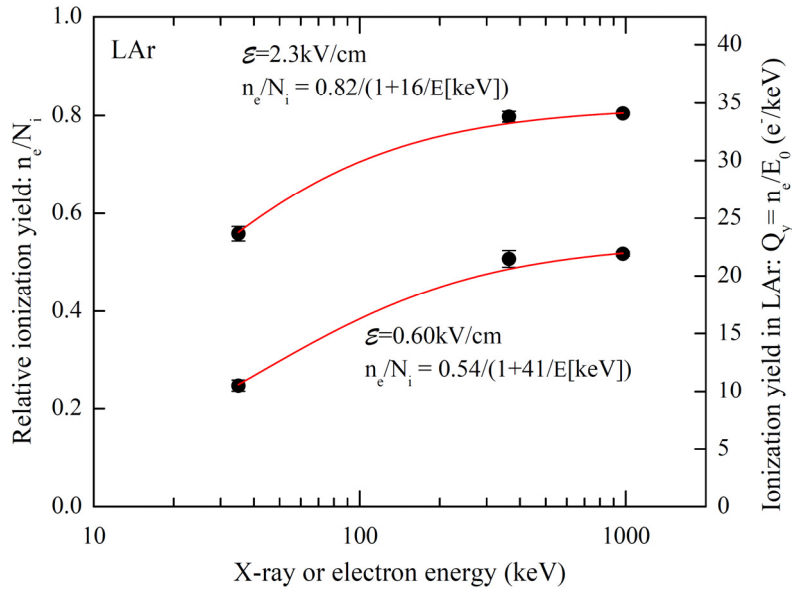


Fig. 6. Relative (left scale) and absolute (right scale) ionization yields in liquid Ar for electron recoils, due to X-ray or electron irradiation, as a function of the X-ray or electron energy, at electric fields of 0.6 and 2.3 kV/cm.

As seen from Table 1, there are only two data points in energy for Ar that can be found in the literature. The third data point is obtained in the current work, in the lower energy domain, from the measurements in the liquid Ar ionization chamber of Fig 1 (left). The result of this measurement is shown in Fig. 4 showing the anode signal charge per X-ray pulse, as a function of the electric field, produced by pulsed X-rays with the average energy of 35 keV (their calculated energy spectrum is shown in Fig. 3). The curve in the figure is the recombination model fit of Eq. (2) to the data points, resulting in the following value of the recombination coefficient: $k=1820\pm110$ V/cm, at the X-ray energy of 35 keV.

In liquid Xe, where there are enough experimental data in the energy range of interest, the relative ionization yield dependence on energy is perfectly described by a function

$$n_e / N_i = a / (1+b/E_0) \quad , \quad (3)$$

with two parameters (a and b): see Fig. 4. Accordingly, in liquid Ar we used the similar function, firstly, to describe the experimental data and, secondly, to extrapolate the data to the energy point of interest.

The results are presented in Figs. 4 and 6 showing the relative (n_e/N_i) and absolute (Q_y) ionization yields in liquid Ar as a function of energy. To obtain the latter, we used a W -value (energy needed to produce one ion pair) and its definition,

$$W = E_0 / N_i \quad ; \quad (4)$$

$W=23.6$ eV for electron recoils in liquid Ar (see table 2 in ref. [2]).

Electric field (kV/cm)	Energy dependence of the relative ionization yield
0.6	$n_e / N_i = 0.54 / (1 + 41\pm5/E_0[\text{keV}])$
1.75	$n_e / N_i = 0.78 / (1 + 20\pm2/E_0[\text{keV}])$
2.3	$n_e / N_i = 0.82 / (1 + 16\pm2/E_0[\text{keV}])$

Table 2. Relative ionization yield dependence on energy in liquid Ar for electron recoils due to X-ray irradiation, at different electric fields used in our experiments.

Electric field (kV/cm)	X-ray energy E_0 (keV)	Number of ionization electrons escaping recombination n_e (e ⁻)	Ionization yield Q_y (e ⁻ /keV)
0.6	59.5	810±40	13.6
1.75	25	460±20	18.4
1.75	59.5	1470±40	24.7
2.3	59.5	1630±50	27.4

Table 3. Number of ionization electrons escaping recombination and absolute ionization yield in liquid Ar for electron recoils due to X-ray irradiation, at different energies and electric fields used in our experiments.

The desired relative ionization yield dependence on energy and the number of ionization electrons escaping recombination in liquid Ar, as well as the absolute ionization yield, at

different electric fields and X-ray energies used in our experiments, are summarized in Tables 2 and 3 respectively. For example, for 59.5 keV X-rays the number of detected ionization electrons in liquid Ar at a field of 1.75 kV/cm is predicted to be $n_e=1470\pm 40 e^-$.

4. Energy spectra

Fig. 3 shows two calculated energy spectra of pulsed X-rays used in the first and second experimental setup; the first spectrum has been already employed in section 3. The second spectrum will be employed in this section.

In the second experimental setup, the multi-channel optical readout of the two-phase CRAD in Ar, using a combined THGEM/GAPD-matrix multiplier, was for the first time demonstrated; the appropriate results were presented in a short paper [12]. The detector had a spatial resolution of 2.5 mm (FWHM), which is rather high for two-phase detectors, and a low detection threshold. In particular, at a rather moderate charge gain, of 160, the yield of the combined THGEM/GAPD-matrix multiplier was claimed to be equal to ~ 80 photoelectrons per 20 keV X-ray absorbed in liquid Ar. In fact, the X-ray energy spectra in liquid Ar were not even presented there [12]. In this section we fill this gap, namely we compare the measured pulsed X-ray energy spectrum to that of calculated in Fig. 3 and thus specify more precisely the energy of the incident X-ray photons. These data are essential for the accurate determination of both the combined multiplier yield and detection threshold of the two-phase CRAD; these will be used in our forthcoming publication [19] where more elaborated results will be presented.

In the case of pulsed X-rays, the X-ray tube was moved away, reaching a relatively large distance (of ~ 50 cm) from the collimator, to provide an operation in X-ray photon counting

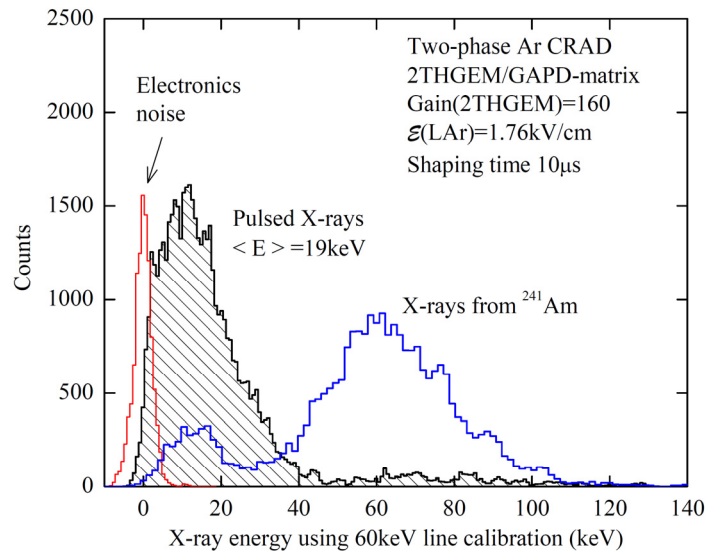


Fig. 7. Energy distributions of charge signals from the double-THGEM in the two-phase CRAD in Ar with 2THGEM/GAPD-matrix multiplier of Fig. 1 (right), at a double-THGEM gain of 160. The signals were induced by X-rays from the ^{241}Am source and pulsed X-ray tube. The energy scale is calibrated using a 60 keV line of the ^{241}Am source. The electric field within liquid Ar was 1.76 kV/cm. The electronic noise pedestal, when the X-rays were off, is also shown.

mode, with a rather small deposited energy per pulse, of the order of 20 keV. The pulsed X-ray energy spectrum measured in these conditions is shown in Fig. 7, along with the electronic noise pedestal and the spectrum from the X-rays of the ^{241}Am source. The latter was used to calibrate the energy scale and to determine the energy resolution, amounting to about $\sigma/E=30\%$, using its 59.5 keV X-ray line. Note that the average energy of the pulsed X-ray spectrum measured using this calibration is equal to 19 keV for the whole spectrum, including the high-energy tail, and to 14 keV for the spectrum peak, when the high-energy tail is disregarded: see Figs. 7 and 8.

In fact, the real energies of the incident pulsed X-ray photons differ from those of “measured”. Indeed, the “measured” pulsed X-ray energy, using the calibration at different energy point, is not equal to its real energy due to the dependence of the X-ray ionization yield on the energy: see Fig. 4 and Table 3. To correctly determine the real X-ray energy, we should compare the predicted spectrum to the measured one. Namely, one should take the calculated spectrum of Fig. 3 and reduce its energy, correcting it for the ionization yield decrease in comparison with that of the energy calibration point (at 59.5 keV). This correction was introduced by the equation $n_e/N_i=0.78/(1+20/E_0[\text{keV}])$ of Table 2, for the electric field of 1.75 kV/cm. In addition, the spectrum should be corrected for the energy resolution contribution ($\sigma/E=30\%$): the spectrum was smeared by a Gaussian distribution using Monte-Carlo simulation.

The result of such corrections is presented in Fig. 8: the measured spectrum is compared to that of calculated for X-ray filtering with 2 mm thick Al and 0.5 mm thick liquid Ar, the latter being corrected for the energy dependence of the ionization yield and the energy resolution. One can see that the simulated spectrum quite well describes the right side and the maximum of the

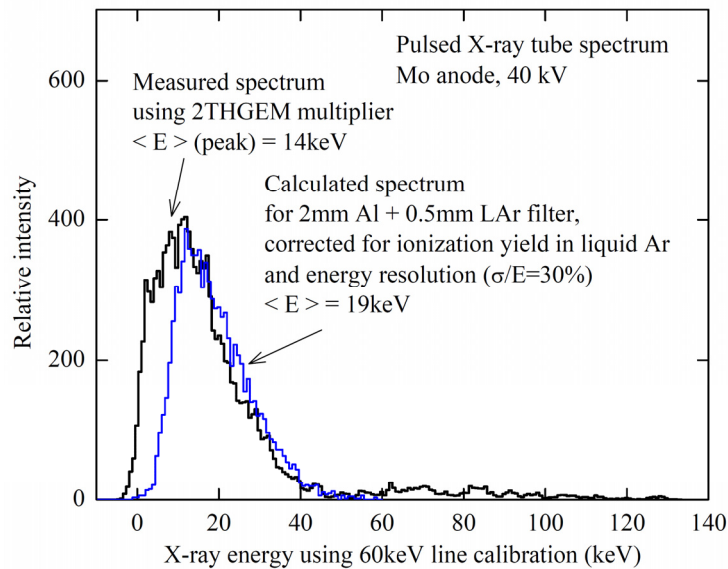


Fig. 8. Energy distributions of charge signals in the two-phase CRAD in Ar with 2THGEM/GAPD-matrix multiplier of Fig. 1 (right) induced by pulsed X-rays. The measurement conditions are those of Fig. 7. The energy scale is calibrated using a 60 keV line of the ^{241}Am source. The measured spectrum is compared to that of calculated for X-ray filtering with 2 mm thick Al and 0.5 mm thick liquid Ar layers. In addition, the calculated spectrum is corrected for the energy dependence of the ionization yield and the energy resolution ($\sigma/E=30\%$).

measured spectrum. On the other hand, the left side of the measured spectrum is enriched with small amplitudes compared to that of simulated: one can see this when comparing the averages of the spectra – 14 keV versus 19 keV. We believe that this is due to the contribution of the secondary soft X-ray photons, due to copious X-ray fluorescence and small-angle scattering of primary X-rays on the inner wall of the collimator. This explanation seems feasible in particular because the collimator is a very narrow, with a high ratio of the wall surface area to the aperture one. With this explanation, the simulated spectrum quite well reproduces the measured one, mostly confirming simulated characteristics of the incident X-ray radiation, with the average energy of 25 keV.

5. Conclusions

In this work we present the results of two related studies. In the first study, we determined the X-ray recombination coefficients and ionization yields in liquid Ar, for the energies and electric fields relevant to our previous [3],[12] and future [19],[20] studies in the field of two-phase CRADs for rare-event experiments, in particular in the energy range of 10-1000 keV and electric fields of 0.6, 1.75 and 2.3 kV/cm.

In the second study, the energy spectra of pulsed X-rays in liquid Ar in the energy range of 15-40 keV, obtained in given experiments including that with the two-phase CRAD, are interpreted and compared to those calculated using a dedicated computer program, to correctly determine the incident X-ray energy.

It should be remarked that the X-ray recombination coefficients and ionization yields have for the first time been presented here for liquid Ar in systematic way. These data might be of particular interest for the energy calibration of dark matter and neutrino detectors using liquid Ar detection medium.

6. Acknowledgements

This work consisted of two independent studies conducted on different experimental setups. The first study was supported by Russian Science Foundation (project N 14-50-00080). The second study was supported by the grants of the Government of Russian Federation (11.G34.31.0047) and Russian Foundation for Basic Research (15-02-01821).

References

- [1] A. Buzulutskov, *Advances in Cryogenic Avalanche Detectors*, 2012 JINST 7 C02025.
- [2] V. Chepel, H. Araujo, *Liquid noble gas detectors for low energy particle physics*, 2013 JINST 8 R04001 [arXiv:1207.2292].
- [3] A. Bondar et al., *Measurement of the ionization yield of nuclear recoils in liquid argon at 80 and 233 keV*, *Europhys. Lett.* 108 (2014) 12001.
- [4] A. Bondar et al., *Two-phase argon and xenon avalanche detectors based on Gas Electron Multipliers*, *Nucl. Instrum. Meth. A* 556 (2006) 273 [arXiv:physics/0510266].

- [5] A. Bondar et al., *Thick GEM versus thin GEM in two-phase argon avalanche detectors*, 2008 JINST 3 P07001 [arXiv:0805.2018].
- [6] A. Bondar et al., *Direct observation of avalanche scintillations in a THGEM-based two-phase Ar avalanche detector using Geiger-mode APD*, 2010 JINST 5 P08002 [arXiv:1005.5216].
- [7] A. Bondar et al., *On the low-temperature performances of THGEM and THGEM/G-APD multipliers in gaseous and two-phase Xe*, 2011 JINST 6 P07008 [arXiv:1103.6126].
- [8] A. Buzulutskov, A. Bondar and A. Grebenuk, *Infrared scintillation yield in gaseous and liquid argon*, Europhys. Lett. 94 (2011) 52001 [arXiv:1102.1825].
- [9] A. Bondar et al., *Study of infrared scintillations in gaseous and liquid argon. Part I: methodology and time measurements*, 2012 JINST 7 P06015.
- [10] A. Bondar et al., *Study of infrared scintillations in gaseous and liquid argon. Part II: light yield and possible applications*, 2012 JINST 7 P06014 [arXiv:1204.0580].
- [11] A. Bondar et al., *Two-phase Cryogenic Avalanche Detectors with THGEM and hybrid THGEM/GEM multipliers operated in Ar and Ar+N₂*, 2013 JINST 8 P02008 [arXiv:1210.0649].
- [12] A. Bondar et al., *First demonstration of THGEM/GAPD-matrix optical readout in two-phase Cryogenic Avalanche Detector in Ar*, Nucl. Instrum. Meth. A 732 (2013) 213 [arXiv:1303.4817].
- [13] Svetlana-X-ray company, <http://svetlana-x-ray.ru>.
- [14] A. Breskin et al., *A concise review on THGEM detectors*, Nucl. Instrum. Meth. A 598 (2009) 107, and references therein.
- [15] D. Renker and E. Lorenz, *Advances in solid state photon detectors*, 2009 JINST 4 P04004, and references therein.
- [16] <http://www.esrf.fr/computing/scientific/xop/>.
- [17] A.S. Barabash, A.I. Bolozdynya, *Liquid ionization detectors*, Energoatomizdat, Moscow, 1993 (in Russian).
- [18] E. Aprile, A. Bolotnikov, A. Bolozdynya, T. Doke, *Noble gas detectors*, WILEY-VCH, Weinheim 2006, and references therein.
- [19] A. Bondar et al., *Study of the combined THGEM/GAPD-matrix multiplier in a two-phase Cryogenic Avalanche Detector in argon*, in preparation.
- [20] A. Bondar et al., *First systematic study of proportional electroluminescence in two-phase argon*, in preparation.
- [21] T.Ya. Voronova et al., *Ionization yield from electron tracks in liquid xenon*, Sov. Phys. Tech. Phys. 34 (1989) 825 [Zh. Tekh. Fiz. 59 (1989) 186].
- [22] E. Shibamura et al., *Drift velocities of electrons, saturation characteristics of ionization and W-values for conversion electrons in liquid argon, liquid argon-gas mixtures and liquid xenon*, Nucl. Instrum. Meth. 131 (1975) 249.
- [23] I.M. Obodovskii and S.G. Pokachalov, *Average ion pair formation energy in liquid and solid xenon*, Sov. J. Low Temp. Phys. 5 (1979) 393.

- [24] D.Yu. Akimov et al., *Experimental study of ionization yield of liquid xenon for electron recoils in the energy range 2.8–80 keV*, 2014 JINST 9 P11014.
- [25] M. Szydagis et al., *Enhancement of NEST capabilities for simulating low-energy recoils in liquid xenon*, 2013 JINST 8 C10003.
- [26] R.T. Scallettar et al., *Critical test of geminate recombination in liquid argon*, Phys. Rev. A 25 (1982) 2419.
- [27] T.H. Joshi et al., *First Measurement of the Ionization Yield of Nuclear Recoils in Liquid Argon*, Phys. Rev. Lett., 112 (2014) 171303.